Journal of Applied Fluid Mechanics, Vol. 14, No. 4, pp. 1269-1282, 2021.
Available online at www.jafmonline.net, ISSN 1735-3572, EISSN 1735-3645.
https://doi.org/10.47176/jafm.14.04.31980

Wave Motion through Mangrove Forests in the Presence of a Viscoelastic Bed due to a Line Source

A. Das[1], S. De[1†] and B. N. Mandal[2]

[1] *Department of Applied Mathematics, University of Calcutta, 92 A.P.C Road, Kolkata-700009, India*
[2] *Physics and Applied Mathematics Unit, Indian Statistical Institute, Kolkata-700108, India*

†*Corresponding Author Email: soumenisi@gmail.com*

(Received July 3, 2020; accepted December 10, 2020)

ABSTRACT

The present paper is concerned with a study of water waves generated due to the presence of a line singularity (source) with time harmonic strength as well as impulsive strength through mangrove forests in the presence of a viscoelastic bed. The trunks of mangroves are assumed to be in the upper layer inviscid fluid, while the roots of mangroves are inside the viscoelastic bed. The equation of motion in the viscoelastic region is obtained by coupling the Voigt's model with the equation of motion in the presence of mangroves. The expressions for the potential functions in the two layers are obtained. The forms of the surface and interface waves are depicted graphically for realistic values of kinematic viscosity and shear modulus of elasticity, the line source being submerged in the upper layer.

Keywords: Wave motion; Mangrove forests; Viscoelastic bed; Line source; Two layer; Muddy bottom.

NOMENCLATURE

V	depth of upper layer	U_x^2	horizontal velocity in lower layer
h_2	depth of viscoelastic layer	U_y^2	vertical velocity in lower layer
g	acceleration due to gravity	ν	kinematic viscocity
f_e	linearising coefficient	σ	angular frequency
G	shear modulas of elasticity	ρ_1	density of upper layer
w_p	peak frequency	ρ_2	density of lower layer
f	depth of the source point	$\Phi_1(x, y)$	velocity potential of upper layer
P_1	hydrodynamic pressure of upper layer	$\Phi_2(x, y)$	velocity potential of lower layer
P_2	hydrodynamic pressure of lower layer	$\Psi_1(x, y)$	stream function of upper layer

1. INTRODUCTION

The study of water wave generation problems by various disturbances present either on the surface or inside the water is of great importance. Velocity potentials due to the presence of various types of singularities commonly known as source potentials have wide applications. If a body is present in water, waves may be generated by the movement of the body. Velocity potentials due to fundamental time harmonic singularities present in an homogeneous, incompressible fluid with a free surface are useful in the investigation of scattering or radiation problems involving obstacles which are either partially immersed or fully submerged in water. These velocity potentials may be identified with the Green's functions for the boundary value problems for solving the Laplace equation subject to appropriate boundary conditions which appear in linear water wave theory. Thorne (1953) listed different kinds of time harmonic singularities present in the fluid. Rhodes-Robinson (1970) modified these results for fluids with surface tension. These time harmonic potential functions are solutions of certain boundary value problems satisfying the Laplace equation in the fluid medium except at a point where a singularity is situated.

The technique of using flow singularities to model floating and submerged bodies has been enormously successful in marine hydrodynamics when irrotational (potential) flow is assumed. Since in inviscid theory the only boundary condition on a solid surface is impermeability, a streamline and a solid surface are one and the same thing. The linearity of the governing equation (Laplace equation) allows one to use a distribution of singularities to satisfy boundary conditions on a solid body, for instance using panel methods. The technique is computationally far cheaper than solving the corresponding boundary value problem with the full equations of motion while still giving satisfactory results for description of wave–body interactions (cf. Newman (2018); Faltinsen (1993)). The submerged oscillatory source is thus recognized as an elementary solution for linearized water waves governed by Laplace equation and the first mathematical solutions were given by Kochin (1952, 1967) also see the review article by Wehausen and Laitone (1960). The linearized water wave radiation problem for an oscillating submerged line source in an inviscid shear flow with a free surface was considered by Ellingsen and Tyvand (2016). The effect of a small undulation at the bottom of a laterally unbounded ocean covered with an ice sheet, on the waves generated by an oscillating line source submerged in water was considered by Banerjea *et al*. (2011). The traditional linearized free-surface conditions were used on both the sea surface and the mudwater interface by Zilman *et al*. (1996). The mud was modeled as a linear viscoelastic substance. The numerical test cases presented in that publication were applicable to an air-cushion vehicle (ACV) traveling over the sea with a muddy bottom, an ACV traveling over mud alone and a ship traveling in a sea with a muddy bottom.

Behera *et al*. (2018) recently have described in some detail the background to model mangrove forests as a fluid layer above a viscoelastic bed while studying wave propagation through mangrove forests. For the sake of completeness, this is also briefly mentioned here. It is widely believed that mangrove forests provide coastal protection and they worked as bio-shields during many marine hazards. After the December 2004 tsunami, a study performed by Kathiresan and Rajendran (2005) in coastal hamlets along the southeast coast of India shows the importance of mangrove forests in coastal area protection. However, some reports state that mangrove forests and tsunami damage has no direct linkage. Gedan *et al*. (2011) concluded that wetlands cannot protect shorelines in all scenarios and some man-made structures are also needed along with the wetlands. Since most of the data based analysis suggests that mangrove forests play a key role in coastal protection, many authors have focused on assessing tsunami wave attenuation and flow patterns around the plants. Physical models such us cylinders, disposed in uniform and organized arrangements have been frequently used to determine dissipation capacity of mangroves. Massel *et al*. (1999) developed a mathematical model to predict the attenuation of wind induced random surface waves in the mangrove forest by replacing the nonlinear term with the linear one. Later, this model was used by Hadi *et al*. (2003) to analyze surface wave attenuation in two types of mangrove forests i.e Rhizophora and Ceriops forests. Both these studies show that the rate of wave energy attenuation depends strongly on the density of the forests, diameter of mangrove roots and trunks. Brinkman (2006) developed a predictive model of propagation through nonuniform forests in water of finite depth. Vo-Luong and Massel (2008) developed a model for arbitrary depth of a nonuniform mangrove forest where they used a modified mild slope equation for modeling the changing water depth within mangrove forest.

Huang *et al*. (2011) investigated the characteristics of the wave height reduction by performing a numerical experiment and simulation regarding the tsunami–vegetation interaction. Ismail *et al*. (2012) tested prototype Rhizophora mangrove forests formed by three different parts: canopy, trunk and root. Their study concretes the fact that their is a strong influence of forest density and width on wave damping. Also Irtem *et al*. (2009) tested cylindrical timber sticks to study tsunami run-up reduction. The same runs were performed considering artificial trees. Tang *et al*. (2013) studied the damping effect on solitary water wave run-up due to vegetated seabed. Their study reveals that vegetation can effectively reduce solitary wave propagation velocity and that solitary wave run-up is decreased with increase of plant height in water and also diameter and stem density. For periodic waves, Mei *et al*. (2014) established the semi-analytical model for predicting the wave attenuation by specific configurations of cylinder array, e.g. an infinitely long forest belt. Liu *et al*. (2015) developed a mathematical model for small-amplitude periodic waves propagating through an aquatic forest within a finite extent. Maza *et al*. (2015) investigated the influence of solitary wave steepness, vegetation density and vegetation arrangement on tsunami wave attenuation using a three dimensional numerical approach based on IHFOAM. Most of these studies focuses on the effects of the vegetation near the shoreline while assuming the bottom surface of the mangrove forest to be an impermeable rigid bed.

When waves are attenuated in coastal waters, the mechanism of energy dissipation generally involves some form of bottom interaction. It is evident that as waves propagate over the sea bed, small deflections can be induced in the sea bed by itself. Associated with such deflections, there is inevitably some dissipation of water wave energy due to internal friction within the sea bed.

To analyze wave attenuation over a region with soft mud bottom Dalrymple and Liu (1978) considered the bottom as a viscous fluid. Later Macpherson (1980) considered the bottom as viscoelastic bed and derived a dispersion relation from which the rates of wave attenuation and sea bed deflections were computed. Hsiao and Shemdin (1980) considered the same problem but in their study they considered the pressure to be continuous. Ng and Zhang (2007), Liu and Chan (2007) contributed notably on the study of water wave propagation over the viscoelastic bed.

Inspired by the success of flow singularities in irrotational flow, we have studied generation of water waves due to the presence of two types of source, one is a time-harmonic line source and another is an impulsive source present in the upper layer consisting of mangrove forests. This can be mathematically viewed as an initial and/or boundary value problem for the potential function (source potential) satisfying Laplace equation in the fluid except at a point where the source is present with appropriate boundary conditions. The lower layer has been considered to be a viscoelastic medium. The expressions for the potential functions in the two layers are determined and the surface and interface profiles are presented graphically. We hope our study will be helpful for further studies on wave attenuation through mangrove forests using linear theory.

2. FORMULATION

A schematic sketch to explain the configuration of the problem is given in the following figure 1. Here the *y*-axis is taken vertically downwards and *x*-axis is in the horizontal direction with $y=0$ representing the mean free surface. The fluid domain consists of a upper layer of homogeneous inviscid water of density ρ_1 and depth h_1 bounded below by a viscoelastic fluid layer of depth h_2 and density ρ_2. It is assumed that the trunks of the mangroves are in the upper layer $(0 < y < h_1)$ while the roots are in the viscoelastic bed $(h_1 < y < h_2)$ which is bounded below by an impermeable rigid flat bottom. The only external force acting on the system is the force due to gravity. The motion in the fluid is generated due to a line singularity in the upper fluid. The mathematical formulation in both the regions is represented as follows (cf. Behera *et al.* (2018)).

Upper region:

The motion in the fluid domain in the upper region is irrotational and incompressible. Thus the velocity potential Φ_1 (for upper region) satisfies the two-dimensional equation

$$\nabla^2\Phi_1 = 0 \tag{1}$$

everywhere except at the point of singularity (0, f), $0 < y < h_1$, $-\infty < x < \infty$, together with the Bernoulli equation

$$\frac{\partial\Phi_1}{\partial t} + f_e w_p \Phi_1 + \frac{P_1}{\rho_1} = g\, y \quad \text{in } 0 < y < h_1, -\infty < x < \infty \tag{2}$$

where P_1 is hydrodynamic pressure, w_p is the peak frequency and f_e is the linearised coefficient associated with the energy dissipation characterized by $f_e w_p \overrightarrow{U_1}$ ($\overrightarrow{U_1}$ is the velocity vector) and g is the acceleration due to gravity. In the calculations of f_e,

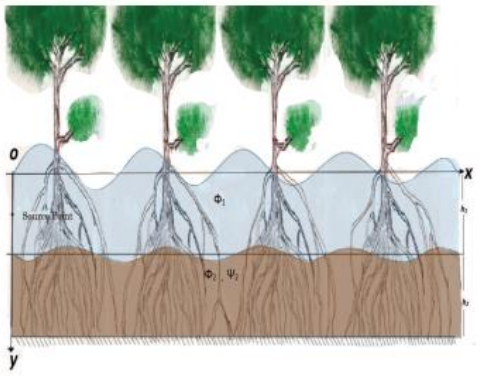

Fig. 1. Configuration of the problem.

the simplified assumption of rigid bottom is used as an alternative of viscoelastic bed, due to the very small value of the linearising coefficient f_e compared to viscous drag inside the viscoelastic layer. The details of the linearisation procedure and determination of the coefficient f_e are given in Appendix B of Massel *et al.* (1999). At the mean free surface $y = 0$, the linearized kinematic condition yields

$$\frac{\partial\eta_1}{\partial t} = \frac{\partial\Phi_1}{\partial y} \quad \text{on} \quad y = 0, \quad -\infty < x < \infty, \tag{3}$$

Where $\eta_1(x,t)$ is the the upper layer surface depression.

The dynamic condition at $y = 0$ yields

$$\frac{\partial\Phi_1}{\partial t} + f_e w_p \Phi_1 = g\eta_1 \quad \text{on} \quad y = 0, \quad -\infty < x < \infty. \tag{4}$$

Combining the kinematic and dynamic condition as in Eqs, (3) and (4) the boundary condition on the mean free surface is obtained as

$$\frac{\partial^2\Phi_1}{\partial t^2} + f_e w_p \frac{\partial\Phi_1}{\partial t} = g\frac{\partial\Phi_1}{\partial y} \quad \text{on} \quad y = 0, \quad -\infty < x < \infty. \tag{5}$$

Lower region:

In the lower layer, the governing equations within the viscoelasatic medium are based on Voigt's model and the main advantage of this is that the governing equations have been reduced to the form of the linearised Navier-Stokes equations for a viscous fluid as discussed in Macpherson (1980). The viscoelastic bed is assumed to be homogeneous in this study. Since this layer is incompressible the linear two dimensional equations for small disturbance in the absence of mangrove may be expressed as

$$\frac{\partial^2\xi^x}{\partial t^2} = -\frac{1}{\rho_2}\frac{\partial^2 P_2}{\partial x^2} + \nu\frac{\partial}{\partial t}\left(\frac{\partial^2\xi^x}{\partial x^2}\right) + \frac{G}{\rho_2}\frac{\partial^2\xi^x}{\partial x^2}, \tag{6}$$

$$\frac{\partial^2 \xi^y}{\partial t^2} = -\frac{1}{\rho_2}\frac{\partial^2 P_2}{\partial y^2} + \nu \frac{\partial}{\partial t}\left(\frac{\partial^2 \xi^y}{\partial y^2}\right) + \frac{G}{\rho_2}\frac{\partial^2 \xi^y}{\partial y^2} + g, \quad (7)$$

where (ξ^x, ξ^y) is the displacement of the particle, P_2 is the pressure distribution, g is the vertical acceleration due to gravity, G is the shear modulus of elasticity and ν is the kinematic viscosity.

In the presence of roots and trunks of the mangroves in this viscoelastic medium, a friction term has to be incorporated in the governing equations as in Hadi *et al*. (2003). The modified governing equations are,

$$\frac{\partial^2 \xi^x}{\partial t^2} = -\frac{1}{\rho_2}\frac{\partial^2 P_2}{\partial x^2} + \nu \frac{\partial}{\partial t}\left(\frac{\partial^2 \xi^x}{\partial x^2}\right) + \frac{G}{\rho_2}\frac{\partial^2 \xi^x}{\partial x^2} - f_e w_p \frac{\partial \xi^x}{\partial t}, \quad (8)$$

$$\frac{\partial^2 \xi^y}{\partial t^2} = -\frac{1}{\rho_2}\frac{\partial^2 P_2}{\partial y^2} + \nu \frac{\partial}{\partial t}\left(\frac{\partial^2 \xi^y}{\partial y^2}\right) + \frac{G}{\rho_2}\frac{\partial^2 \xi^y}{\partial y^2} - f_e w_p \frac{\partial \xi^y}{\partial t} + g \quad (9)$$

where f_e, w_p are defined earlier.

Continuity equation is given by

$$\frac{\partial U_2^x}{\partial x} + \frac{\partial U_2^y}{\partial y} = 0 \quad (10)$$

where $U_2 = (U_2^x, U_2^y)$ is the velocity component in the lower region. Now, within the viscoelastic medium, the particle velocities can be expressed in terms of scalar functions $\Phi_2(x, y, t)$ and $\Psi_2(x, y, t)$ given by (cf. Lamb (1932))

$$U_2^x = \frac{\partial \Phi_2}{\partial x} + \frac{\partial \Psi_2}{\partial y} \text{ and } U_2^y = \frac{\partial \Phi_2}{\partial y} - \frac{\partial \Psi_2}{\partial x}. \quad (11)$$

Here Φ_2 denotes the velocity potential and Ψ_2 denotes the stream function.Moreover, the linearized Bernoulli equation of this region is analogous to that of upper region and can be written as

$$\frac{\partial \Phi_2}{\partial t} + \frac{P_2}{\rho_2} + f_e w_p \Phi_2 = gy \quad \text{in } h_1 < y < h_2, -\infty < x < \infty \quad (12)$$

where P_2 is the pressure within this region. It may be mentioned that the Bernoulli equation relates the velocity potential with pressure, the pressure depends only on Φ_2, it does not depend on Ψ_2. As the velocity is continuous at the interface, the linearized kinematic condition at the mean interface is given by

$$\frac{\partial \eta_2}{\partial t} = U_1^y = U_2^y \quad \text{on } y = h_1, -\infty < x < \infty, \quad (13)$$

where U_1 and U_2 are the corresponding vertical velocities of upper layer and lower layer. Expressing the velocities in terms of scalar function, we have,

$$\frac{\partial \eta_2}{\partial t} = \frac{\partial \Phi_2}{\partial y} - \frac{\partial \Psi_2}{\partial x} = \frac{\partial \Phi_1}{\partial y} \quad \text{on } y = h_1 - \infty < x < \infty, \quad (14)$$

where η_2 is the viscoelastic bed depression. In the absence of surface tension normal stress at the mean viscoelatic bed $y = h_1$ must be continuous. Therefore

$$\left(P_2 - 2\rho_2 \nu_s \frac{\partial U_2^y}{\partial y}\right) - P_1 = 0 \text{ on } y = h_1,$$

so that

$$P_2 - P_1 = 2\rho_2 \nu_s \frac{\partial U_2^y}{\partial y} \quad \text{on } y = h_1. \quad (15)$$

The vanishing of the shear stress yields

$$\frac{\partial U_2^x}{\partial y} + \frac{\partial U_2^y}{\partial x} = 0 \quad \text{on } y = h_1. \quad (16)$$

Eliminating the pressure and velocity terms by the scalar functions, we get

$$2\frac{\partial^2 \Phi_2}{\partial x \partial y} + \frac{\partial^2 \Psi_2}{\partial y^2} - \frac{\partial^2 \Psi_2}{\partial x^2} = 0 \quad \text{on } y = h_1. \quad (17)$$

$$\left(\rho_2 \frac{\partial \Phi_2}{\partial t} - \rho_1 \frac{\partial \Phi_1}{\partial t}\right) + 2\rho_2 \nu_s \left(\frac{\partial^2 \Phi_2}{\partial y^2} - \frac{\partial^2 \Psi_2}{\partial x \partial y}\right) + f_e w_p (\rho_2 \Phi_2 - \rho_1 \Phi_1) = g(\rho_2 - \rho_1)\eta_2 \quad \text{on } y = h_1. \quad (18)$$

The final condition, vanishing of the horizontal and vertical velocities at the rigid horizontal bed is given by

$$\frac{\partial \Phi_2}{\partial x} + \frac{\partial \Psi_2}{\partial y} = 0 \text{ and } \frac{\partial \Phi_2}{\partial y} - \frac{\partial \Psi_2}{\partial x} = 0 \quad \text{on } y = h_1 + h_2. \quad (19)$$

3. METHOD OF SOLUTION

Case - 1 (Time harmonic source)

Here, it is assumed that a time harmonic line source is present at the point (0, f). Therefore,

$$\Phi_1 \to \log r e^{-i\sigma t} \text{ as } r = \sqrt{x^2 + y^2} \to 0, \quad (20)$$

Then the motion can be considered to be simple harmonic with frequency σ, so that the velocity potentials (of the upper and lower fluids) are time harmonic too. Therefore, Eq. (5) can be written as

$$\frac{\partial \phi_1}{\partial y} = -\frac{\sigma^2}{g}(1 + i f_e w_p)\phi_1 \quad \text{on } y = 0, \quad -\infty < x < \infty. \quad (21)$$

where $\Phi_1 = Re[\phi_1 e^{-i\sigma t}]$. The frequencies σ and w_p are different in general. The complex valued potential ϕ_1 satisfies the Laplace equation

$$\nabla^2 \phi_1 = 0 \tag{22}$$

By virtue of the time harmonic property of the motion, Eqs. (8) and (9) can be further simplified as

$$\frac{\partial U_2^x}{\partial t} = -\frac{1}{\rho_2}\frac{\partial P_2}{\partial x} + \nu_s \nabla^2 U_2^x - f_e w_p U_2^x, \tag{23}$$

$$\frac{\partial U_2^y}{\partial t} = -\frac{1}{\rho_2}\frac{\partial P_2}{\partial y} + \nu_s \nabla^2 U_2^y - f_e w_p U_2^y + g \tag{24}$$

where $(U_2^x, U_2^y) = \left(\frac{\partial \xi^x}{\partial t}, \frac{\partial \xi^y}{\partial t}\right)$ is the velocity vector of the viscoelastic fluid particle and $\nu_s = \nu + i\frac{G}{\sigma\rho_2}$. Using Eqs. (11) in Eqs. (10), (23) and (24), the governing equations of motion can be expressed in terms of scalar functions $\Phi_2(x,y,t)$ and $\Psi_2(x,y,t)$ as

$$\nabla^2 \Phi_2 = 0 \text{ and } \nu_s \nabla^2 \Psi_2 = \frac{\partial \Psi_2}{\partial t} + f_e w_p \Psi_2. \tag{25}$$

Since the scalar functions $\Phi_2(x,y,t)$ and $\Psi_2(x,y,t)$ are time harmonic with frequency σ these equation reduce to

$$\nabla^2 \phi_2 = 0 \text{ and } \nabla^2 \psi_2 = \alpha \psi_2, \tag{26}$$

where $\Phi_2 = Re[\phi_2 e^{-i\sigma t}], \Psi_2 = Re[\psi_2 e^{-i\sigma t}]$ and $\alpha = \frac{f_e w_p - i\sigma}{\nu_s}$. The details of this derivation is provided in the Appendix of Behera *et al*. (2018).

Introducing a characteristic length h, characteristic time $\sqrt{\frac{h}{g}}$, we define the dimensionless quantities as,

$$\bar{x} = \frac{x}{h}, \bar{y} = \frac{y}{h}, \bar{t} = t\sqrt{\frac{g}{h}}, \bar{t} = \frac{t}{h}, \overline{h_1} = \frac{h_1}{h}, \overline{h_2} = \frac{h_2}{h},$$

$$\overline{\phi_i} = \frac{\phi_i}{h\sqrt{gh}}, \bar{\psi} = \frac{\psi}{h\sqrt{gh}}, s = \frac{\rho_1}{\rho_2},$$

$$\bar{f} = \frac{f}{h}, \bar{G} = \frac{G}{\rho_2 g h}, \bar{\nu} = \frac{\nu}{\sqrt{gh^3}}$$ Using the fact that $\Phi_i = Re[\phi_i e^{-i\sigma t}], \Psi_2 = Re[\psi_2 e^{-i\sigma t}]$ and removing the bars, the dimensionless quantities satisfy

$$\nabla^2 \phi_1 = 0 \quad \text{for } 0 < y < h_1, -\infty < x < \infty \tag{27}$$

everywhere except at the point of singularity $(0, f)$,

$$\frac{\partial \phi_1}{\partial y} = -\sigma^2(1 + i f_e w_p)\phi_1 \quad \text{on } y = 0 \quad -\infty < x < \infty, \tag{28}$$

$$\nabla^2 \phi_2 = 0 \text{ for } h_1 < y < h_2, \ -\infty < x < \infty, \tag{29}$$

$$\nabla^2 \psi_2 = \alpha \psi_2 \text{ for } h_1 < y < h_2, \ -\infty < x < \infty, \tag{30}$$

$$\frac{\partial \phi_2}{\partial y} - \frac{\partial \psi_2}{\partial x} = \frac{\partial \phi_1}{\partial y} \text{ on } y = h_1, \tag{31}$$

$$2\frac{\partial^2 \phi_2}{\partial x \partial y} + \frac{\partial^2 \psi_2}{\partial y^2} - \frac{\partial^2 \psi_2}{\partial x^2} = 0 \quad \text{on } y = h_1, -\infty < x < \infty, \tag{32}$$

$$(s-1)\frac{\partial \phi_1}{\partial y} - \sigma^2\left(1 + i\frac{f_e w_p}{\sigma}\right)(\phi_2 - s\phi_1) + 2\nu_s(-i\sigma)\left(\frac{\partial^2 \phi_2}{\partial y^2} - \frac{\partial^2 \psi_2}{\partial x \partial y}\right) = 0 \text{ on } y = h_1, \tag{33}$$

$$\frac{\partial \phi_2}{\partial x} + \frac{\partial \psi_2}{\partial y} = 0 \text{ and } \frac{\partial \phi_2}{\partial y} - \frac{\partial \psi_2}{\partial x} = 0 \text{ on } y = h_1 + h_2. \tag{34}$$

To solve the boundary value problem governed by the Eqs. (27), (29) and (30), the velocity potential can be expressed following Thorne (1953) as

$$\phi_1 = log\frac{r}{r_1} + \int_0^\infty [A(k)\cosh k(h_1 - y) + B(k)\sinh ky]\cos kx dk, \tag{35}$$

$$\psi_2 = \int_0^\infty [E(k)\cosh l(h_1 + h_2 - y) + F(k)\sinh l((h_1 + h_2 - y))]\sin kx dk, \tag{36}$$

$$\phi_2 = \int_0^\infty [G(k)\cosh k(h_1 + h_2 - y) + H(k)\sinh k((h_1 + h_2 - y))]\cos kx dk \tag{37}$$

where $l = \sqrt{k^2 + \alpha}$, $r_1 = \sqrt{x^2 + (y + f)^2}$. Using the boundary conditions (34) ϕ_2 can be written as

$$\phi_2 = \int_0^\infty [-\left(\frac{l}{k}\right)F(k)\cosh k(h_1 + h_2 - y) - F(k)\sinh k((h_1 + h_2 - y))]\cos kx dk \tag{38}$$

Here *A(k), B(k), E(k), F(k)* are unknown functions and are determined by using the boundary conditions.

Condition (32) yields

$$E(k) = -\frac{(l^2 + k^2)\sinh lh_2 - 2lk\sinh kh_2}{(l^2 + k^2)\cosh lh_2 - 2k^2\cosh kh_2}F(k). \tag{39}$$

From (28) we obtain,

$$A(k) = \frac{k}{k\sinh kh_1 - \sigma^2\left(1 + i\frac{f_e w_p}{\sigma}\right)\cosh kh_1}B(k) - \frac{2e^{-kf}}{k\sinh kh_1 - \sigma^2\left(1 + i\frac{f_e w_p}{\sigma}\right)\cosh kh_1}. \tag{40}$$

Finally, we obtain

$$\phi_1 = log\frac{r}{r_1} + \int_0^\infty \frac{a(k)\cosh k(h_1-y)+b(k)\sinh k\,y}{\Delta(k)v(k)}\cos kx\,dk. \tag{41}$$

Where

$$a(k)=\alpha\Big(l\sinh kh_2\cosh lh_2 - k\sinh lh_2\cosh kh_2\Big)\Big(2s\sigma^2\Big(1+i\frac{f_e w_p}{\sigma}\Big)\sinh k(f-h_1)-2(s-1)k\cosh k(f-h_1)\Big)-2k\cosh k(f-h_1)\Big(A\cosh kh_2\cosh lh_2 - B\sinh kh_2\sinh lh_2 + C\Big),$$

$$b(k)=\alpha\Big(l\sinh kh_2\cosh lh_2 - k\sinh lh_2\cosh kh_2\Big)\Big(2s\sigma^2\Big(1+i\frac{f_e w_p}{\sigma}\Big)e^{-kf}+2\sigma^2\Big(1+i\frac{f_e w_p}{\sigma}\Big)\times se^{-kh_1}\sinh kf-2(s-1)e^{-kh_1}\sinh kf\Big) +2\{B\sinh kh_2\sinh lh_2 - A\cosh kh_2\cosh lh_2 - C\}e^{-kh_1}\sinh kf,$$

$$\Delta(k)=s\alpha\sigma^2\Big(1+i\frac{f_e w_p}{\sigma}\Big)kl\sinh kh_2\cosh lh_2 +(s-1)\alpha kl\cosh kh_1\sinh kh_2\cosh lh_2 + s\sigma^2\times\Big(1+i\frac{f_e w_p}{\sigma}\Big)l\alpha\sinh kh_1\sinh kh_2\cosh lh_2 - s\sigma^2\Big(1+i\frac{f_e w_p}{\sigma}\Big)k^2\alpha\sinh lh_2\cosh kh_2 n\times\cosh kh_1 - s\sigma^2\Big(1+i\frac{f_e w_p}{\sigma}\Big)k\alpha\sinh kh_1 n\times\sinh lh_2\cosh kh_2 + kcoshkh_1(A\cosh kh_2 n\times\cosh lh_1 - B\sinh kh_2\sinh lh_2 + C),$$

With

$$A=\sigma^2\Big(1+i\frac{f_e w_p}{\sigma}\Big)\times(l^2+k^2)\frac{l}{k}-2\nu_s(-i\sigma)kl(l^2+3k^2),$$

$$B=\sigma^2\Big(1+i\frac{f_e w_p}{\sigma}\Big)\times(l^2+k^2)-2\nu_s(-i\sigma)k^2(3l^2+k^2),$$

$$C=2\nu_s(-i\sigma)kl(l^2+3k^2)-2\sigma^2\Big(1+i\frac{f_e w_p}{\sigma}\Big)lk,$$

$$v(k)=k\sinh kh_1-\sigma^2\Big(1+i\frac{f_e w_p}{\sigma}\Big)\cosh kh_1$$

and

$$\phi_2 = 2s\sigma^2\Big(1+i\frac{f_e w_p}{\sigma}\Big)\Big(\int_0^\infty \frac{\sinh k(h_1+h_2-y)}{\Delta(k)v(k)}\times\cos kx(k\cosh k(f-h_1)-\sinh kf\,v(k))((l^2+k^2)\times\sinh lh_2-2kl\sinh kh_2)dk - \int_0^\infty \frac{\cosh k(h_1+h_2-y)\cos kx}{k\Delta(k)v(k)}\times(kl\cosh k(f-h_1)+lv(k)\sinh kf)((l^2+k^2)\times\cosh lh_2-2k^2\cosh kh_2)dk\Big), \tag{42}$$

$$\psi_2 = 2s\sigma^2(1+i\frac{f_e w_p}{\sigma})\Big(\int_0^\infty \frac{\sinh l(h_1+h_2-y)}{\Delta(k)v(k)}\times\cos kx(k\cosh k(f-h)-v(k)\sinh kf)((l^2+k^2)\times\cosh lh_2-2k^2\cosh kh_2)dk - \int_0^\infty \frac{\cosh l(h_1+h_2-y)}{\Delta(k)v(k)}\times\cos kx(k\cosh k(f-h)+v(k)\sinh kf)((l^2+k^2)\times\sinh lh_2-2kl\sinh kh_2)dk\Big). \tag{43}$$

From the normalized form of the Eq. (4), the normalized surface elevation is obtained as

$$\eta_1(x,t)=Re\Big[(f_e w_p-i\sigma)\int_0^\infty\Big(2\alpha(l\sinh kh_2\cosh lh_2-k\sinh lh_2\cosh kh_2)(s\sigma^2\Big(1+i\frac{f_e w_p}{\sigma}\Big)\sinh k(f-h_1)-(s-1)k\times\cosh k(f-h_1))-2k\cosh k(f-h_1)(A\cosh kh_2\cosh lh_2-B\sinh kh_2\sinh lh_2+C)\Big)\frac{\cosh kh_1\cos kx}{\Delta(k)v(k)}\,dk\;e^{-i\sigma t}\Big]. \tag{44}$$

Normalized interface elevation h2 can be computed from the equation

$$\eta_2(x,t)=Re\Big[\frac{1}{(s-1)}\Big(\frac{\partial\Phi_2}{\partial t}-s\frac{\partial\Phi_1}{\partial t}+2\nu_s(\frac{\partial^2\Phi_2}{\partial y^2}-\frac{\partial^2\Psi_2}{\partial x\partial y})+f_e w_p(\Phi_2-s\Phi_1)\Big)\Big](x,h_1,t). \tag{45}$$

Case-2(Source of impulsive strength)

Here it is considered that a line source of impulsive strength is present at (0,*f*). Therefore

$$\Phi_1\to\delta(t)\log r \text{ as } r=\sqrt{x^2+y^2}\to 0. \tag{46}$$

The initial conditions are given by

$$\Phi_i=0,\Psi_2=0,\frac{\partial\Phi_i}{\partial t}=0,\frac{\partial\Psi_2}{\partial t}=0,\text{at } t=0. \tag{47}$$

Let, $\tilde{\phi}_i(x,y,p)=\int_0^\infty \Phi_i(x,y,t)e^{-pt}dt$ and

$\tilde{\psi}_2(x,y,p)=\int_0^\infty \Psi_2(x,y,t)e^{-pt}dt$ be the Laplace transforms of Φ_i,Ψ_2 respectively. Taking Laplace transform of non-dimensional form of Eq. (1), (5), (46) and (11), we have

$$\nabla^2\,\tilde{\phi}_1=0 \text{ for } 0<y<h_1\,,-\infty<x<\infty \tag{48}$$

everywhere except at the point of singularity (0,*f*),

$$\frac{\partial\tilde{\phi}}{\partial y}=p(p+f_e w_p)\tilde{\phi} \quad \text{on } y=0\ -\infty<x<\infty, \tag{49}$$

$$\tilde{\phi}_1\to\log r \text{ as } r=\sqrt{x^2+y^2}\to 0, \tag{50}$$

$$\tilde{U}_2^x=\frac{\partial\,\tilde{\phi}_2}{\partial x}+\frac{\partial\tilde{\psi}_2}{\partial y} \text{ and } \tilde{U}_2^y=\frac{\partial\,\tilde{\phi}_2}{\partial y}-\frac{\partial\,\tilde{\psi}_2}{\partial x}, \tag{51}$$

where $\tilde{U}_2^x$ and $\tilde{U}_2^y$ are the Laplace transform of U_2^x and U_2^y respectively. Now, Eq. (8) can be written as

$$\frac{\partial U_2^x}{\partial t}=-\frac{1}{\rho_2}\frac{\partial P_2}{\partial x}+\nu\nabla^2U_2^x +\frac{G}{\rho_2}\nabla^2\Big(\int_0^t U_2^x(t')dt'\Big)-f_e w_p U_2^y. \tag{52}$$

Taking Laplace transform of Eq. (52) we have

$$p\tilde{U}_2^x=-\frac{1}{\rho_2}\frac{\partial\tilde{P}_2}{\partial x}+\nu\nabla^2\tilde{U}_2^x +\frac{G}{\rho_2}\nabla^2\Big(\frac{1}{p}\tilde{U}_2^x\Big)-f_e w_p\tilde{U}_2^x. \tag{53}$$

Similarly, Laplace transform of Eq. (9) yields

$$p\;\tilde{U}_2^x=-\frac{1}{\rho_2}\frac{\partial\,\tilde{P}_2}{\partial x}+\;\tilde{\nu}_s\nabla^2\tilde{U}_2^x-f_e w_p\;\tilde{U}_2^x \tag{54}$$

where $\tilde{\nu}_s=\nu+\frac{G}{\rho_2 p}$. Introducing the scalar functions from Eq. (51) into Eqs. (53) and (54) we have

$$\nabla^2\tilde{\phi}_2=0 \text{ and } \tilde{\nu}_s\nabla^2\tilde{\psi}_2=\tilde{\alpha}\;\tilde{\psi}_2$$

where $\tilde{\alpha}=\frac{f_e w_p+p}{\tilde{\nu}_s}$. Taking Laplace transform of non-dimensional form of Eq. (14), (17), (18) and (19) we get

$$\frac{\partial\tilde{\phi}_2}{\partial y}-\frac{\partial\,\tilde{\psi}_2}{\partial x}=\frac{\partial\tilde{\phi}_1}{\partial y} \text{ on } y=h_1,\ -\infty<x<\infty, \tag{56}$$

$$2\frac{\partial^2\tilde{\phi}_2}{\partial x\partial y}+\frac{\partial^2\psi\tilde{\psi}_2}{\partial y^2}-\frac{\partial^2\tilde{\psi}_2}{\partial x^2}=0 \quad \text{on } y=h_1,-\infty<x<\infty, \tag{57}$$

$$(s-1)\frac{\partial\tilde{\phi}_1}{\partial y}-p(p+f_e w_p)\big(\tilde{\phi}_2-s\tilde{\phi}_1\big) +2\tilde{\nu}_s p\left(\frac{\partial^2\tilde{\phi}_2}{\partial y^2}-\frac{\partial^2\tilde{\psi}_2}{\partial x\partial y}\right)=0 \text{ on } y=h_1, \tag{58}$$

$$\frac{\partial\tilde{\phi}_2}{\partial x}+\frac{\partial\tilde{\psi}_2}{\partial y}=0 \text{ and } \frac{\partial\tilde{\phi}_2}{\partial y}-\frac{\partial\tilde{\psi}_2}{\partial x}=0 \quad \text{on } y=h_1+h_2. \tag{59}$$

Clearly, $\tilde{\phi}_1$, $\tilde{\phi}_2$ and $\tilde{\psi}_2$ satisfies the equations quite similar to the complex valued potentials associated with the time harmonic case. So, as described earlier, we can write the solutions as

$$\tilde{\phi}_1=\log\frac{r}{r_1}+\int_0^\infty\frac{u(k)\cosh k(h_1-y)+w(k)\sinh k\,y}{\Delta_1(k)v_1(k)}\cos kx\,dk, \tag{60}$$

where

$$u(k)=2\tilde{\alpha}\Big(l\sinh kh_2\cosh lh_2-k\sinh lh_2\cosh kh_2\Big)\Big((1-s)k\cosh k(f-h_1)-sp(p+f_e w_p)\sinh k(f-h_1)\Big)-2k\cosh k(f-h_1)\Big(M\cosh kh_2\cosh lh_2+N\sinh kh_2\sinh lh_2+Q\Big),$$

$$w(k)=2\alpha\Big(l\sinh kh_2\cosh lh_2-k\sinh lh_2\cosh kh_2\Big)\Big(e^{-kh_1}\sinh kf\Big((1-s)-sp(p+f_e w_p)\Big)-se^{-kf}\,p(p+f_e w_p)\Big)-2\{M\cosh kh_2\cosh lh_2+N\sinh kh_2\sinh lh_2+Q\}e^{-kh_1}\sinh kf,$$

$$\Delta_1(k)=(s-1)\tilde{\alpha}kl\cosh kh_1\sinh kh_2\cosh lh_2-s\tilde{\alpha}\,p(p+f_e w_p)kl\sinh kh_2\cosh lh_2+sp(p+f_e w_p)k^2\tilde{\alpha}\sinh lh_2\cosh kh_2\times\cosh kh_1-sp(p+f_e w_p)l\tilde{\alpha}\sinh kh_1\sinh kh_2\cosh lh_2+sp(p+f_e w_p)k\tilde{\alpha}\sinh kh_1\times\sinh lh_2\cosh kh_2+k\cosh kh_1(M\cosh kh_2\times\cosh lh_1+N\sinh kh_2\sinh lh_2+Q)$$

with

$$M=2\tilde{\nu}_s pkl(l^2+3k^2)-p(p+f_e w_p)\times(l^2+k^2)\frac{l}{k},$$

$$dN=p(p+f_e w_p)(l^2+k^2)+2\nu_s pk^2(3l^2+k^2)$$

$$Q=2\tilde{\nu}_s pkl(l^2+3k^2)+2p(p+f_e w_p)lk,$$

$$v_1(k)=k\sinh kh_1+p(p+f_e w_p)\cosh kh_1$$

And

$$\tilde{\phi}_2=2\mathrm{sp}(\mathrm{p}+\mathrm{f_e w_p})\int_0^\infty\frac{\cosh\mathrm{k}(\mathrm{h}_1+\mathrm{h}_2-\mathrm{y})\cos\mathrm{kx}}{\mathrm{k}\Delta_1(\mathrm{k})\mathrm{v}_1(\mathrm{k})}\times(\mathrm{kl}\cosh\mathrm{k}(\mathrm{f}-\mathrm{h}_1)+\mathrm{lv}_1(\mathrm{k})\sinh\mathrm{kf})((\mathrm{l}^2+\mathrm{k}^2)$$

$$\times\cosh lh_2 - 2k^2\cosh kh_2)dk - 2sp(p+f_e w_p)$$
$$\int_0^\infty \frac{\sinh k(h_1+h_2-y)}{\Delta_1(k)v_1(k)}\cos kx(v(k)\sinh kf \quad (61)$$
$$+k\cosh k(f-h_1))((l^2+k^2)\sinh lh_2$$
$$-2kl\sinh kh_2)dk,$$

$$\tilde{\psi}_2 = 2sp(p+f_e w_p)\int_0^\infty \frac{\cosh l(h_1+h_2-y)}{\Delta(k)v(k)}$$
$$\times\cos kx(k\cosh k(f-h_1)+v(k)\sinh kf)((l^2+k^2) \quad (62)$$
$$\times\sinh lh_2 - 2kl\sinh kh_2)dk - 2sp(p+f_e w_p)$$
$$\int_0^\infty \frac{\sinh l(h_1+h_2-y)}{\Delta(k)v(k)}\cos kx(k\cosh k(f-h_1)$$
$$+v(k)\sinh kf)((l^2+k^2)\cosh lh_2 - 2k^2\cosh kh_2)dk.$$

Therefore, the free surface elevation is given by

$$\eta_1(x,t) = \frac{1}{2\pi i}\int_{c-i\infty}^{c+i\infty}\int_0^\infty \Big(2\alpha(l\sinh kh_2\cosh lh_2$$
$$-k\sinh lh_2\cosh kh_2)((1-s)k\cosh k(f-h_1)$$
$$-sp(p+f_e w_p)\sinh k(f-h_1)\cosh k(f-h_1))$$
$$-2k\cosh k(f-h_1)(M\cosh kh_2\cosh lh_2 \quad (63)$$
$$+N\sinh kh_2\sinh lh_2 + Q)\Big)$$
$$\frac{(p+f_e w_p)\cosh kh_1\cos kx}{\Delta(k)v(k)}e^{pt}\,dp\,dk$$

and similarly the expression for $\eta_2(x,t)$ can be obtained from (18) after taking the Laplace inverse of the potential functions. The integrals arising during the computation are multiple integrals which can be evaluated approximately by the method of steepest-descent (cf. Jeffreys and Lapwood (1957)). Usually the use of the method of steepest-descent for a single integral requires a large parameter in the exponential term of the integrand.

However, Jeffreys and Lapwood (1957)obtained steepest-descent approximations of multiple integrals whose integrands do not necessarily have any large parameter explicitly in the exponential term.

4. NUMERICAL RESULTS

The roots of the dispersion equation for the wave propagation through mangrove forests with viscoelastic bottom are all complex in nature. Only two roots lie close to the positive real axis which contributes to the propagation of surface and interface waves. The detailed analysis of the position the roots is discussed by Behera *et al.* (2018). The outgoing waves at surface and interface are studied for various values of linearising factor, shear modulus of elasticity and kinematic viscosity for different positions of the source. The quantities $\eta_i, x, t, f, \nu, G, f_e$ v have already been non dimensionalised.

All the figures have been drawn taking h_1 =1; h_2 =2.5; G =1.27; ν =2; f_e = 0.15; f =0.375; t = 5 . It is to be noted here the non-dimensional value G=1.27 corresponds to a value of 10^5 Newton/m^2 and the non-dimensional value ν =2 corresponds to approximately the value of 50 m^2/sec. All the values have been taken as mentioned above unless otherwise stated.

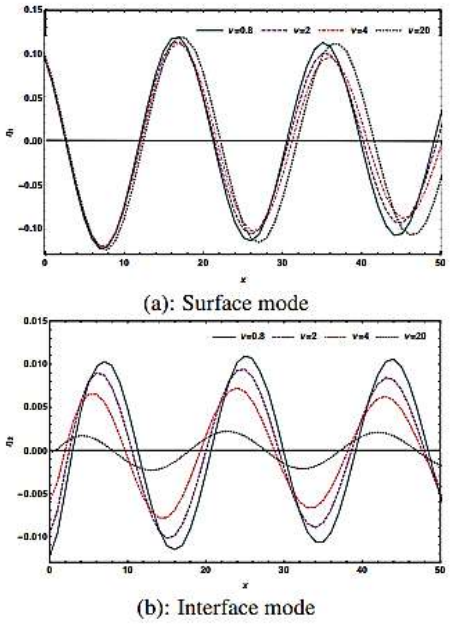

Fig. 2. Normalized response amplitude in surface and interface modes for different values of n against *x*.

Case-I ($f_e << 1$)

Figures 2-5 represent η when the presence of mangrove is negligible i.e the factor of drag force is very small. This is the case of a two-layer system with the lower layer as a viscoelastic medium. Figure 2 represents η for various values of ν , ν =0.8, 2, 4, 20. It is observed that with the increase of ν the height of peak of surface waves increases but height of peak of interface waves decreases. Figure 3 represents the surface mode (Fig.3a) and interface mode (Fig.3b) for different positions of the source. When the source is present nearer to the free surface, it causes waves of greater amplitude. Figure 4 is for different values of *G*. Graphs for *G* = 1.27, 1.9, 2.5, 5 have been drawn here. Greater values of *G* causes greater height of peak at the surface but lesser height of peak at the interface.

The depth of the viscoelastic layer also affects the damping of the waves which can be seen in Fig. 5. When the density of the lower layer is taken to be 1.25 times the density of the water, graphs of free surface elevation have been drawn for h_2 =1.25, 1.75, 2.5, 3.75. Figure 4(b) represents the interface mode of the above situation.

Case-II $(G = 0)$

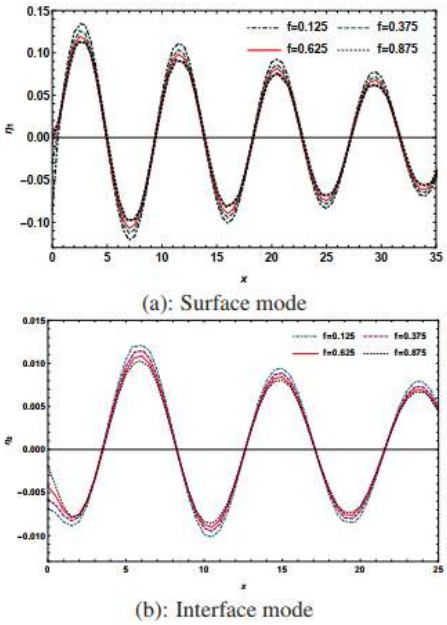

Fig. 3. Normalized response amplitude in surface and interfacemodes for different values of *f* against *x*.

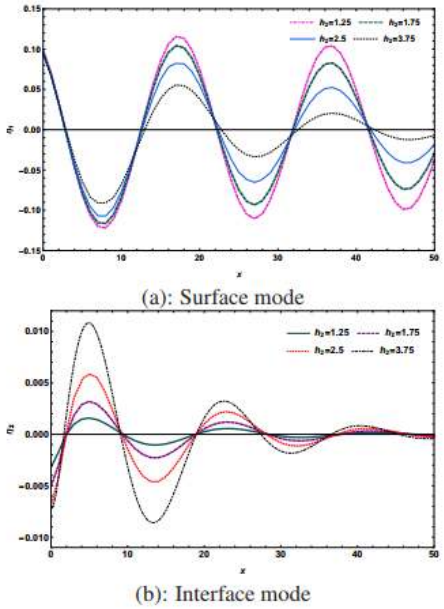

Fig. 5. Normalized response amplitude in surface and interface modes for different values of h_2 against *x*.

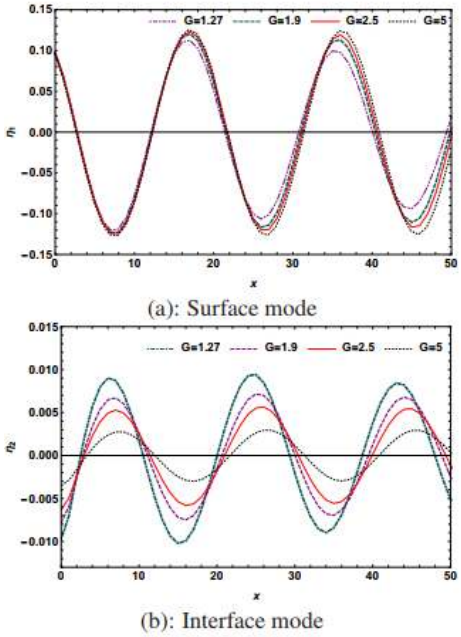

Fig. 4. Normalized response amplitude in surface and interface modes for different values of *G* against *x*.

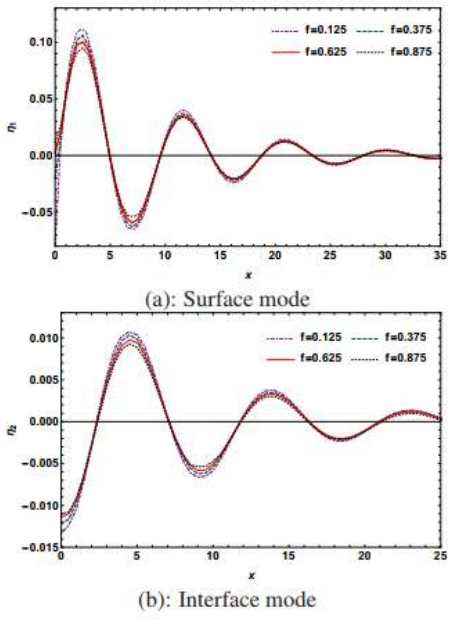

Fig. 6. Normalized response amplitude in surface and interface modes for different values of *f* against *x*.

Here the lower medium has been taken as a viscous medium instead of a viscoelastic medium. Figure 6 represents waves at surface and interface respectively for non-dimensional *f*=0.125, 0.375, 0.625, 0.875. It is observed that when the source is nearer to the free surface the particles nearer to the source are displaced more than the particles at large distances. In fact at a large distance the variations are almost negligible. Figure 7 represents η_1 and η_2 for different values of ν, the larger values causes greater height of peak at surface but lesser height of peak at interface. Figure 8 depicts the waves at surface and interface for different values of f_e. The denser forests prohibit the motion of outgoing waves. Generally, the value of f_e lies in the interval (0.05, 0.35). The different curves represent the waves

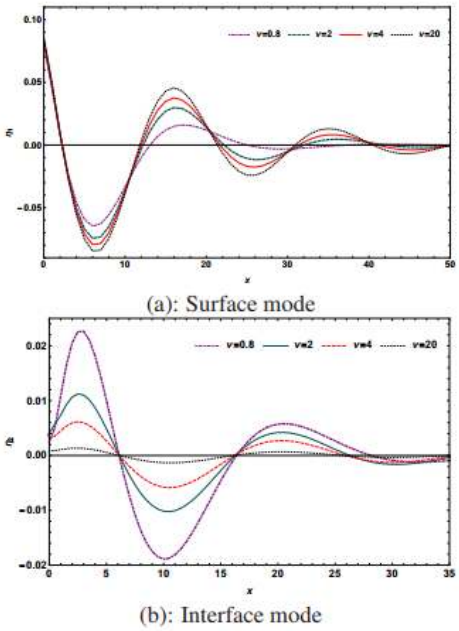

Fig. 7. Normalized response amplitude in surface and interface modes for different values of n against *x*.

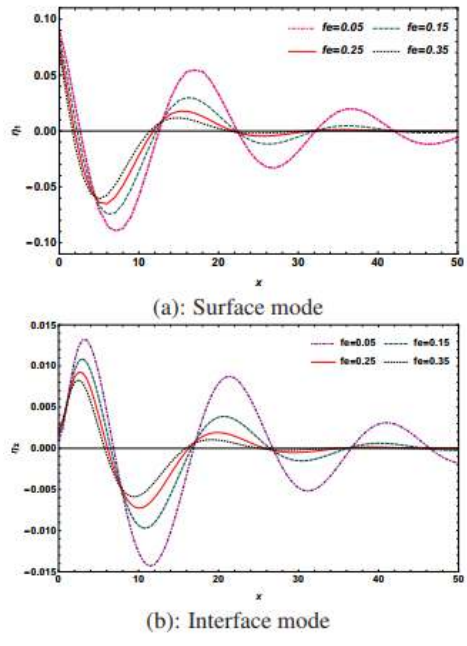

Fig. 8. Normalized response amplitude in surface and interface modes for different values of f_e against *x*.

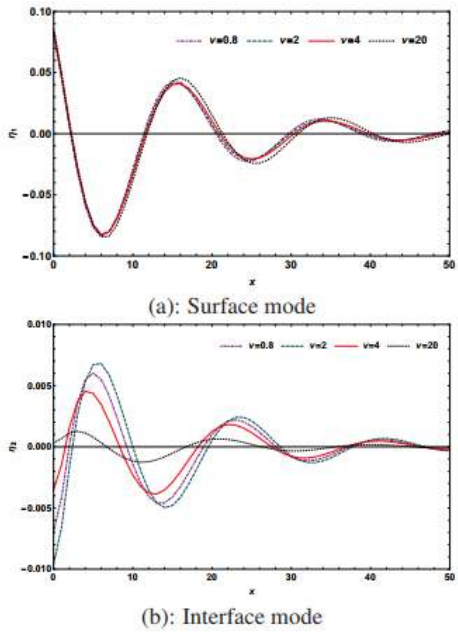

Fig. 9. Normalized response amplitude in surface and interface modes for different values of n against *x*.

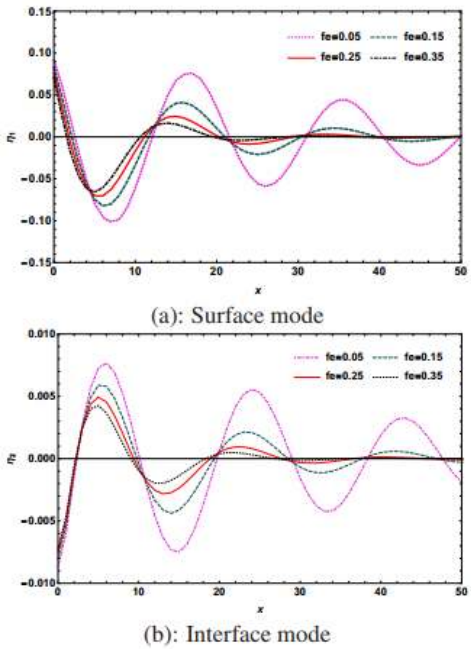

Fig. 10. Normalized response amplitude in surface and interface modes for different values of f_e against *x*.

for f_e = 0.5, 0.15, 0.25, 0.35. Increasing values of f_e causes the waves to diminish faster.

Case-III

Here the waves at surface and interface have been represented graphically for mangrove forests with viscoelastic bed. Figures 9-12 represent η_1 and η_2 for variation in different parameters. Figures 9(a) and 9(b) depict η_1 and η_2 for variation in ν. Similar results have been observed. Figure 10 is for different density of forests. Graphs have been drawn for different values of f_e. Similar to the previous cases Fig. 11 shows that smaller values of *f* causes greater

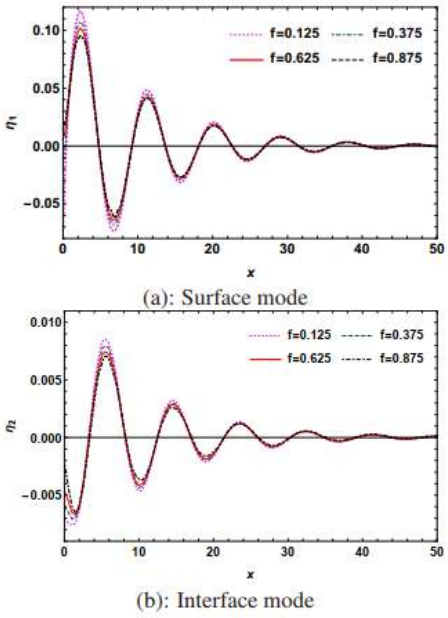

Fig. 11. Normalized response amplitude in surface and interface modes for different values of *f* against *x*.

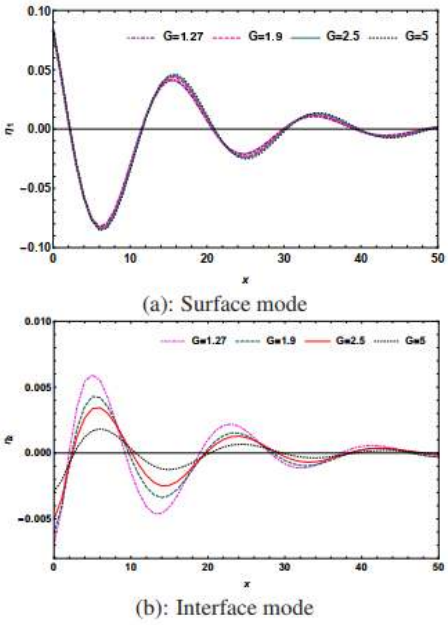

Fig. 12. Normalized response amplitude in surface and interface modes for different values of *G* against *x*.

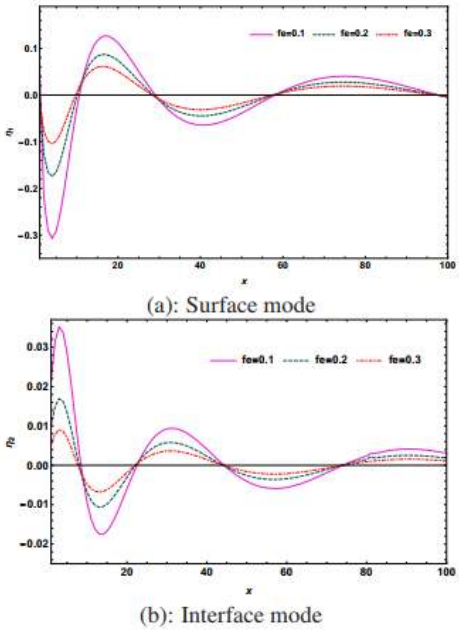

Fig. 13. Normalized response amplitude in surface and interface modes for different values of f_e against *x* at t=6.

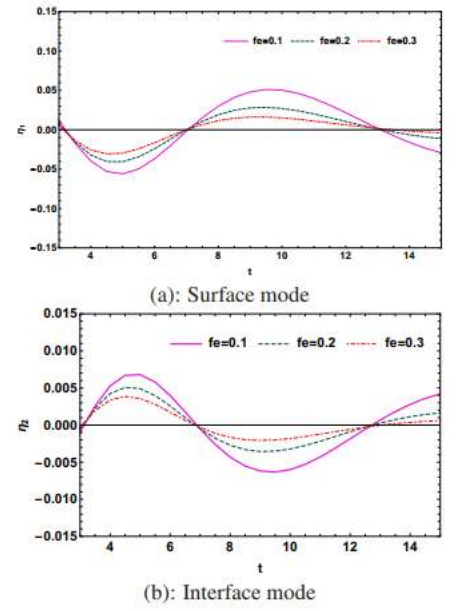

Fig. 14. Normalized response amplitude in surface and interface modes for different values of *fe* against *t* at x=50.

height of peak but at larger distances the waves become similar. Figure 12 shows the effects of variation in *G*.

Case-IV

Here the source is considered to be of impulsive strength. Figure 13 represents the wave profiles for different values of f_e at t =6. It can observed that the effect of the forest density is quite similar to the previous cases i.e the amplitude of the waves gets diminished as the waves gets deeper into the forest. As the density of the forest increases the attenuation rate is much faster. Figure 14 and Fig. 15 depict the variation in the wave amplitude with time. In Fig. 14, the normalized wave amplitudes have been plotted against time for x =50 and similar plots have been depicted for x =75 in Fig. 15. Both these figures show the decrease in amplitude with time and the

rapid decease in amplitude for denser forest over time.

Finally, Fig. 16 represents the amplitude ratio vs kinematic viscosity graph for different values of *G*. In this figure, the values of *G* and $\mathcal{V}$ are taken as dimensional.

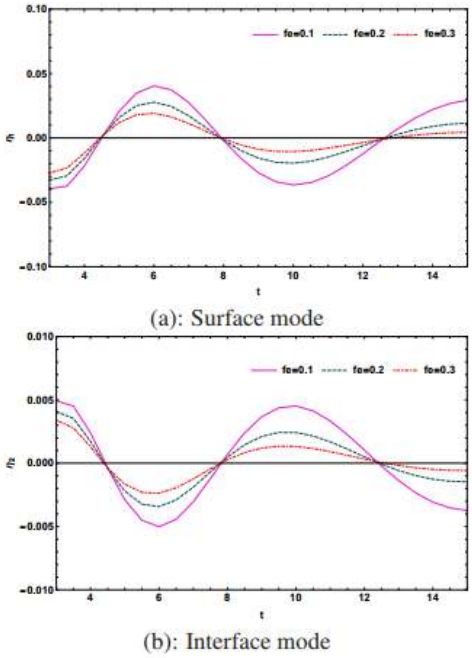

Fig. 15. Normalized response amplitude in surface and interface modes for different values of *fe* against *t* at x=75.

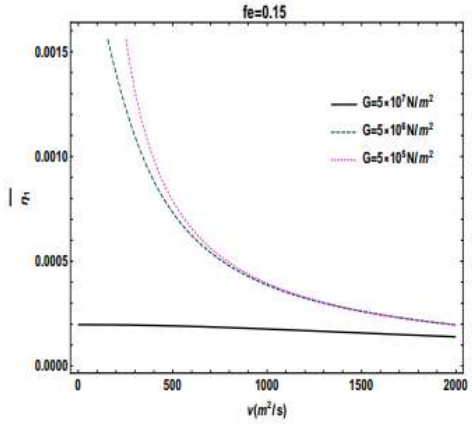

Fig. 16. Amplitude ratio against kinematic viscosity for different values of G.($\mathcal{V}$ and *G* have dimensional value in this figure).

5. DISCUSSION

The effects of mangrove trunks and viscoelastic bed on the surface waves and interface waves due to the presence of a line singularity submerged in water is studied here. Since the lower medium is considered to be viscoelastic the wave at interface is the deformation at the muddy layer.

Numerical computations show that in the absence of mangrove, lower values of shear modulus of elasticity causes waves of lesser amplitude at the surface. As the elasticity increases, value of η_1 also increases. These waves are progressive and oscillatory in nature. But at interface an opposite phenomenon has been noticed. In the absence of shear modulus of elasticity the deformation in the lower medium is greater than the case when elasticity is present and for greater value of shear modulus of elasticity the amplitude of the interface wave is decreasing. In the absence of mangroves the position of the source plays a major role for the amplitude of the surface and interface waves. Source nearer to the free surface is creating larger waves relative to the waves generated by a source nearer to the interface. At large distances, the variation is very small, but here we have noticed that for lesser angular frequency this variation for different positions of source point is very small. The effect of kinematic viscosity on the free surface wave in the absence of mangrove is very prominent, the lower viscosity helps the surface wave to damp faster. In the presence of mangrove the effect of damping is more faster. At the interface the effect of viscosity is more prominent. As the viscosity increases, the amplitude is getting smaller and smaller and for very large values of viscosity the deformation is too negligible that it can be considered as almost rigid bottom. In the presence of mangroves the amplitude ratio shows that as the viscosity increases the ratio decreases rapidly because as the viscosity increases the waves at surface has greater amplitude but the interface has lesser amplitude. We also notice that the elastic effects of the bed has similar effect. For higher values of kinematic viscosity the effect of elasticity is not prominent but the for lower viscosity this effect is very significant. The presence of elasticity decreases the amplitude of waves at the interface. In the absence of shear modulus of elasticity as there are no elastic forces to restore the bed to its undisturbed state the waves at the interface have greater amplitude in the absence of elastic forces.

In the case of a body or a number of bodies undergoing small oscillations in fluid medium waves of small amplitudes are generated. If the motion starts initially from rest then it can be assumed to be irrotational and thus it can be described uniquely by a velocity potential. As the motion is of small amplitude the basic equations of linearised theory involving the velocity potential can be assumed to hold good. When a body or a number of bodies are present the resulting motion of the fluid can be described by a series of singularities placed on the body or bodies. These singularities are characterised by their giving rise to velocity potentials which are typical singular solutions of Laplace equation in the neighbourhood of the singularity. For two dimensional problems, these singularities are of logarithmic types or multipole types and for three dimensional problems these are point sources or multipoles. Thus the determination of velocity potentials due to different types of singularities in a

fluid medium is of considerable importance and has important application in the mathematical study of many real life physical phenomena describing the wave propagation in ocean. Usually, the ocean is modeled as a fluid medium with a free surface of infinite or finite depth. For a fluid medium with infinite depth or uniform finite depth these potentials are well known (cf. Thorne (1953), Wehausen and Laitone (1960),Rhodes-Robinson (1970). For a two-fluid medium these were obtained by Gorgui and Kassem (1978),Rhodes-Robinson (1980), Mandal (1981), Kassem (1982). However, for mangrove forests modeled as a two-layer fluid with a viscoelastic bed these potentials are yet to be determined. Thus the problem of determination of source potential due to a line source in mangrove forests appears to be quite important both mathematically and physically as it has application in real life physical phenomena involving wave propagation through a medium such as coastal mangroves.

ACKNOWLEDGMENTS

The authors thank the Reviewers for their comments and suggestions to revise the paper in the present form. AD thanks the UGC, India, for providing financial support (File number: F.16-6(DEC. 2016)/2017(NET)), as a research scholar of the University of Calcutta, India. This work is also supported by SERB through the research project No. EMR/2016/005315.

REFERENCES

Banerjea, S., P. Rakshit and P. Maiti (2011). On the waves generated due to a line source present in an ocean with an ice cover and a small bottom undulation. *Fluid Dynamics Research* 43, 025506.

Behera, H., S. Das and T. Sahoo (2018). Wave propagation through mangrove forests in the presence of a viscoelastic bed. *Wave Motion* 78, 162–175.

Brinkman, R. M. (2006). *Wave attenuation in mangrove forests: an investigation through field and theoretical studies*. Ph. D. thesis, James Cook University.

Dalrymple, R. A. and P. L. F. Liu (1978). Waves over soft muds: a two-layer fluid model. *Journal of Physical Oceanography* 8, 1121–1131.

Ellingsen, S. Å and P. A. Tyvand (2016). Oscillating line source in a shear flow with a free surface: critical layer-like contributions. *Journal of Fluid Mechanics* 798, 201–231.

Faltinsen, O. (1993). *Sea Loads on Ships and Offshore Structures*. Cambridge University Press.

Gedan, K. B., M. L. Kirwan, E. Wolanski, E. B. Barbier and B. R. Silliman (2011). The present and future role of coastal wetland vegetation in protecting shorelines: answering recent challenges to the paradigm. *Climatic Change* 106, 7–29.

Gorgui, M. and S. Kassem (1978). On the generation of short internal waves by cylinders oscillating at the surface separating two infinite liquids. *Mathematical Proceedings of the Cambridge Philosophical Society* 83, 481–494.

Hadi, S., H. Latief and M. Muliddin (2003). Analysis of surface wave attenuationin mangrove forests. *Journal of Engineering and Technological Sciences* 35, 89–108.

Hsiao, S. and O. Shemdin (1980). Interaction of ocean waves with a soft bottom. *Journal of Physical Oceanography* 10, 605–610.

Huang, Z., Y. Yao, S. Y. Sim and Y. Yao (2011). Interaction of solitary waves with emergent, rigid vegetation. *Ocean Engineering* 38, 1080–1088.

Irtem, E., N. Gedik, M. S. Kabdasli and N. E. Yasa (2009). Coastal forest effects on tsunami run-up heights. *Ocean Engineering* 36, 313–320.

Ismail, H., A. Abd Wahab, and N. E. Alias (2012). Determination of mangrove forest performance in reducing tsunami run-up using physical models. *Natural Hazards* 63, 939–963.

Jeffreys, H. and E. Lapwood (1957). The reflexion ofa pulse within a sphere.*Proceedingsof the Royal Society of London. Series A. Mathematical and Physical Sciences* 241, 455–479.

Kassem, S. E. (1982). Multipole expansions for two superposed fluids, each of finite depth. *MathematicalProceedingsof the Cambridge Philosophical Society* 91, 323–329.

Kathiresan, K. and N. Rajendran (2005). Coastal mangrove forests mitigated tsunami. *Estuarine, Coastal and Shelf Science* 65, 601–606.

Kochin, N. E. (1952). *The two-dimensional problem of the steady oscillations of bodies under the free surface of a heavy incompressible liquid*. Society of Naval Architects and Marine Engineers.

Kochin, N. E. (1967). *The theory of waves generated by oscillations of a body under the free surface of a heavy incompressible fluid*. Society of Naval Architects and Marine Engineers.

Lamb, H. (1932). *Hydrodynamics*. Cambridge University Press.

Liu, P. L. F. and I. C. Chan (2007). On longwave propagation over a fluid-mud seabed. *Journal of Fluid Mechanics* 579, 467–480.

Liu, P. L. F., C. W. Chang, C. C. Mei, P. Lomonaco, F. L. Martin and M. Maza (2015). Periodic water waves through an aquatic forest. *Coastal Engineering* 96, 100– 117.

Macpherson, H. (1980).The attenuationof water waves over a non-rigid bed. *Journal of Fluid Mechanics* 97, 721–742.

Mandal, B. N. (1981). Some basic singularities in the theory of internal waves in a two-fluid medium in the presence of surface tension. *Journal of Technology* 26, 11–22.

Massel, S., K. Furukawa and R. Brinkman (1999). Surface wave propagation in mangrove forests. *Fluid Dynamics Research* 24, 219 – 249.

Maza, M., J. L. Lara and I. J. Losada (2015). Tsunami wave interaction with mangrove forests: A 3-D numerical approach. *Coastal Engineering* 98, 33–54.

Mei, C. C., I. C. Chan and P. L. F. Liu (2014). Waves of intermediate length through an array of vertical cylinders. *Environmental Fluid Mechanics* 14, 235–261.

Newman, J. N. (2018). *Marine hydrodynamics*. The MIT press.

Ng, C. O. and X. Zhang (2007). Mass transport in water waves over a thin layer of soft viscoelastic mud. *Journal of Fluid Mechanics* 573, 105–130.

Rhodes-Robinson, P. F. (1970). Fundamental singularities in the theory of water waves with surface tension. *Bulletin of the Australian Mathematical Society* 2, 317–333.

Rhodes-Robinson, P. F. (1980). On waves at an interface between two liquids. *Mathematical Proceedings of the Cambridge Philosophical Society* 88, 183–191.

Tang, J., D. Causon, C. Mingham and L. Qian (2013).Numericalstudy of vegetationdamping effects on solitary wave run-up using the nonlinear shallow water equations. *Coastal Engineering* 75, 21–28.

Thorne, R. (1953). Multipole expansions in the theory of surface waves. *Mathematical Proceedings of the Cambridge Philosophical Society* 49, 707–716.

Vo-Luong, P. and S. Massel (2008). Energy dissipation in non-uniform mangrove forests of arbitrary depth. *Journal of Marine Systems* 74, 603–622.

Wehausen, J. V. and E. V. Laitone (1960). Surface waves. In *Fluid Dynamics/Strömungsmechanik*, pp. 446–778. Springer.

Zilman, G., T. Miloh, and L. Doctors (1996). The influence of a bottom mud layer on the resistance of marine vehicles. *Ship Technology Research* 43, 51–61.